Jurnal Mekanikal
December 2006, No. 22, 64-74

ESTIMATION OF AERODYNAMIC CHARACTERISTICS OF A LIGHT AIRCRAFT

Iskandar Shah Ishak*
Shabudin Mat
Tholudin Mat Lazim
Mohd. Khir Muhammad
Shuhaimi Mansor
Mohd Zailani Awang

Faculty of Mechanical Engineering
Universiti Teknologi Malaysia
81310 UTM Skudai, Johor
Malaysia

ABSTRACT

This paper presents the aerodynamic estimation carried out on a three-dimensional aircraft model by conducting wind tunnel tests and Computational Fluid Dynamics (CFD) simulation. The test model is a 15% scaled down from a two-seater light aircraft that is closed to the Malaysian made SME MD3-160 aircraft. This aircraft model has been tested at two different low speed tunnels, namely at Universiti Teknologi Malaysia's tunnel (UTM-LST) test section sized of 2.0 x 1.5 m^2, and at Institute Aerodynamic Research, National Research Council of Canada (IAR-NRC) sized 3.0 x 2.0 m^2 tunnel. The speed during testing at UTM-LST and IAR-NRC tunnels was up to 70 m/s, which corresponds to Reynolds Number of 1.3 x 10^6. The longitudinal and lateral directional aerodynamic characteristics of the aircraft such as coefficients of pressure, forces (lift, drag and side force) and moments (roll, pitch and yaw moment) had been experimentally measured either using direct force measurement or pressure measurement method. The data reduction methods included the strut support interference factor using dummy image and the blockage correction had been applied in this wind tunnel tests. On top of the experimental study, simulation was also performed using a commercial CFD code, FLUENT. Experimental works at UTM-LST and IAR–NRC tunnel showed that the aerodynamic characteristics of this light aircraft were in good agreement with each other. Simultaneously, the aerodynamic forces obtained from the experimental works and CFD simulations had been compared. The results proved that they were agreeable especially at a low angle of attack.

Keywords: *Aerodynamic studies, wind tunnel tests, data reduction methods and CFD simulation.*

1.0 INTRODUCTION

Nowadays, the implementation of wind tunnel tests and simulation by CFD is a must in the stage of the design analysis process. This paper will present the wind

* Corresponding author: E-mail: shah@fkm.utm.my, Tel: +607-5534664, Fax: +607-5566159

tunnel testing technique on a 15% scaled-down model of two-seater light aircraft and its data reduction procedures in order to estimate the aircraft's aerodynamic characteristics. CFD simulation is also carried out for comparison purposes.

2.0 EXPERIMENTAL STUDY

A 15% scaled down model of two-seater light aircraft that has close resemblance to the Malaysian made SME MD3-160 has been selected for the experiment. The aircraft model is equipped with control surfaces such as flaps, aileron, rudder and elevator and it is designed for pressure measurement testing and direct force measurement using a 6-components balance system. The testing was previously conducted at IAR/NRC (in Spring of 2000) and later at UTM-LST (in October 2002). For the data reduction process, corrections have been made for wind tunnel flow angularity (including balance misalignment), blockage, buoyancy, wall interference and STI (Strut, Tare and Interference) corrections. The following discussion is based on the testing conducted at UTM-LST.

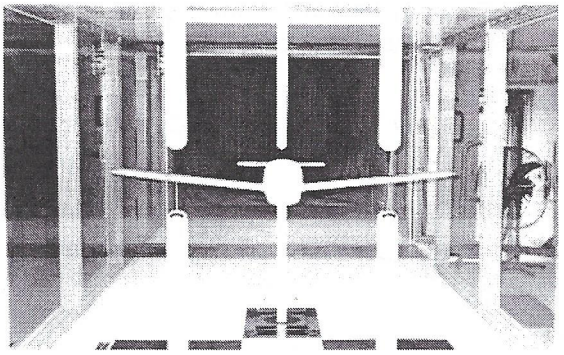

Figure 1: Wind tunnel testing at UTM-LST

2.1 Wind Tunnel Flow Angularity Correction

This correction is to remove the effects of the wind tunnel flow angularity (upwash) and any misalignment between the balance lift vector and the free stream. In order to assess these effects, a model is run upright and inverted with main struts and dummy struts installed. The two runs are over plotted and the corrections to α becomes apparent since in an ideal tunnel, the two runs should overlay each other.

These two curves are parallel but offset by 0.52°. As shown in Barlow [1], the correction is equal to half of the angle offset which is 0.26°. Therefore the model-upright data needs to have 0.26° added to the incidence angle and the model-inverted data needs to have 0.26° subtracted. The measured drag also needs to be corrected. This arises because the non-orthogonality of the lift vector to the flow means that a small component of the measured lift is actually drag. As shown in Barlow, the additive correction to drag coefficient for an upright model is $\Delta C_D = C_L * \tan(\alpha_{up})$ which in this case, α_{up} is 0.26°.

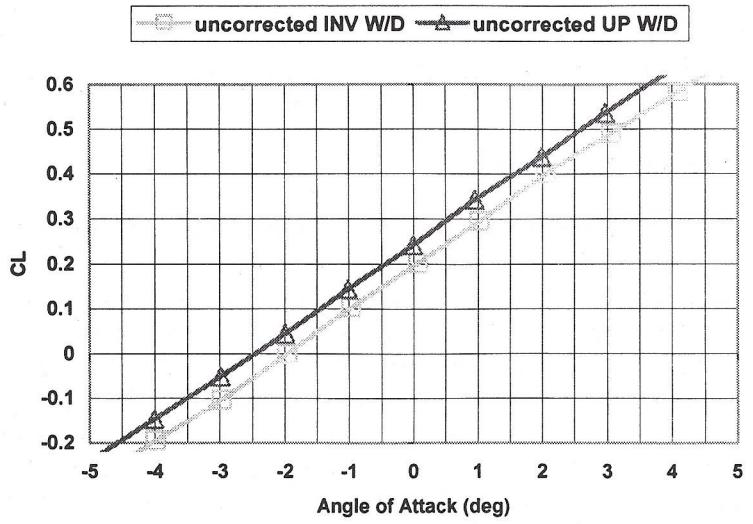

Figure 2: Results from upright and inverted pitch runs, main dummies installed

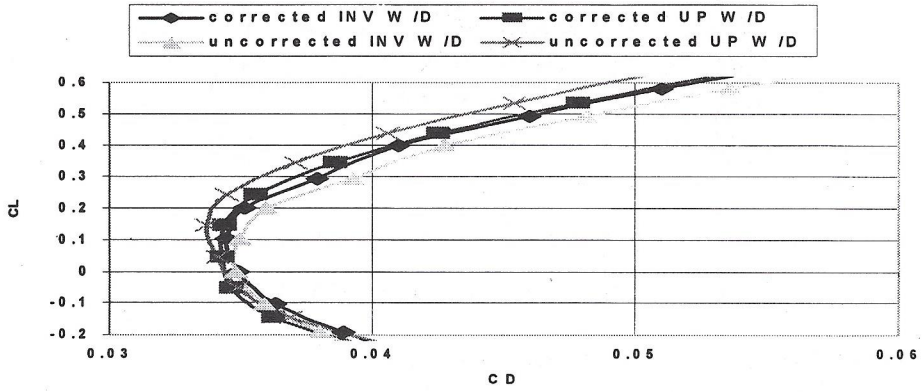

Figure 3: Implementation of flow up wash correction to drag polar

2.2 Blockage Correction

In preparation for removal of blockage and buoyancy effects, the data are converted to wind axis. Lift and yawing moment are unchanged. With the subscripts **W** for wind axis and **S** for stability axis, and ψ defined as positive to the right when viewed from above, the remaining equations are:

$$C_{YW} = C_{YS} \cos\psi - C_{DS} \sin\psi$$

$$C_{DW} = C_{DS} \cos\psi + C_{YS} \sin\psi$$

$$C_{mW} = C_{mS} \cos\psi + C_{lS} \sin\psi * (b/c)$$

$$C_{lW} = C_{lS} \cos\psi - C_{mS} \sin\psi * (c/b)$$

The premise of the corrections is based on a perturbation velocity ε such that the corrected velocity, V_C, can be determined from the uncorrected velocity, V_U, as follows [6]:

$$V_C = V_U*(1+\varepsilon) \quad \text{where} \quad \varepsilon = \varepsilon_{sb} + \varepsilon_{wb}$$

ε_{sb} = Solid blockage

ε_{wb} = Wake blockage

The rest of the equations are [6]:

$$q_c = q_u [1 + (2 - M^2) \varepsilon]$$

$$M_c = M_u [1 + (1 + 0.2 M^2) \varepsilon]$$

$$T_c = T_u (1 - 0.4M^2\varepsilon)$$

$$P_c = P_u (1\text{-}1.4M^2\varepsilon)$$

$$\rho_c = \rho_u (1 - M^2\varepsilon)$$

2.3 Buoyancy Correction

Before correcting the aerodynamic loads due to the effects of blockage, any buoyancy effects are removed from the wind axis drag.

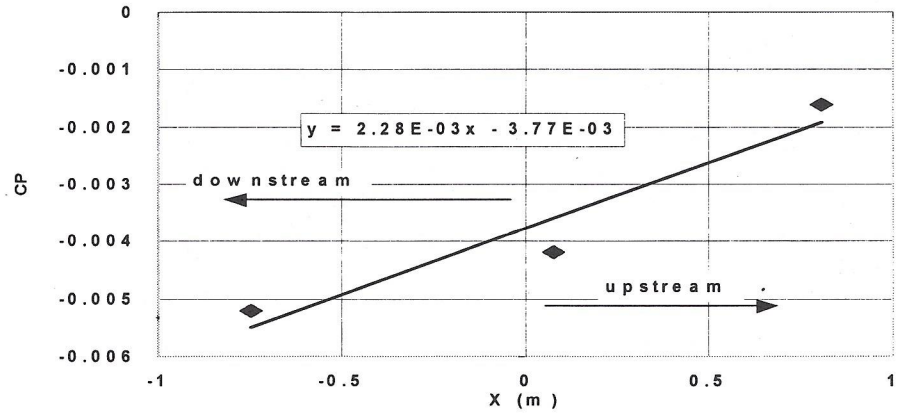

Figure 4: Static pressure gradient in empty test section of UTM-LST

The buoyancy can be expressed as :

$$\Delta C_D = dC_p/dx*(V/S)$$

where S is the wing area and V is the fuselage volume

It is found that the buoyancy correction for the model under test is only about 1 drag count (ΔC_D = 0.0001). With the completion of the corrections which are wind-axes based, the results can be transformed back to stability axes as follows (C_L and C_n are unchanged) :

$$C_{YS} = C_{YW} \cos\psi + C_{DW} \sin\psi$$

$$C_{DS} = C_{DW} \cos\psi - C_{YW} \sin\psi$$

$$C_{mS} = C_{mW} \cos\psi - C_{lW} \sin\psi*(b/c)$$

$$C_{lS} = C_{lW} \cos\psi + C_{mW} \sin\psi*(c/b)$$

2.4 Corrections for Wall Interference

These corrections typically represent some of the largest corrections applied to 3D aircraft models. The corrections arise because of the reflection of the wing tip vortices in the tunnel walls, floor and ceiling.

2.5 STI Corrections

The STI corrections are applied as the final correction of this data reduction. Data for STI were collected for a pitch run only at α= -15°, 0° and +15° owing to current UTM-LST limitations.

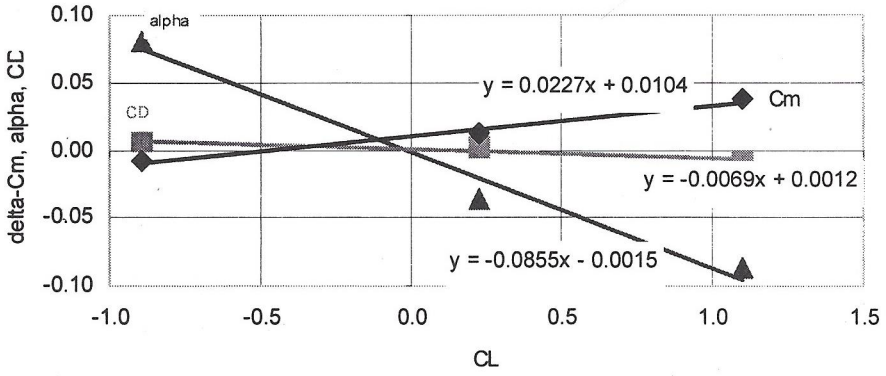

Figure 5: STI corrections

STI corrections as developed by subtracting "all dummy inverted" data from "no dummy inverted" data that will need to be subtracted from "no dummy upright" data.

3.0 CFD SIMULATION

For a comparison purpose, simulation was done at a grace of a commercial CFD code, Fluent. A simplified 15% scaled model is simulated at Reynolds Number of

1.3×10^6 with a speed of 70 m/s. In this project, the simulations were carried out at two different number of elements (with angle of attack varies from 0^0 to 15^0 at an interval of 5^0) using k-epsilon standard. For the first simulation, the model was simulated at 230,000 elements whereas the second simulation was at 300,000 elements. Results for both simulations were then compared for comparison purposes. This is to ensure that the aerodynamic forces obtained from this study are free from the elements factor. Figure 6 gives a comparison results for both simulations.

Angle of Attack	C_L	
	Simulation 1 230k elements	Simulation 2 300k elements
0°	0.1990	0.2016
5°	0.6588	0.6601
10°	1.0649	1.0611
15°	1.2985	1.2983

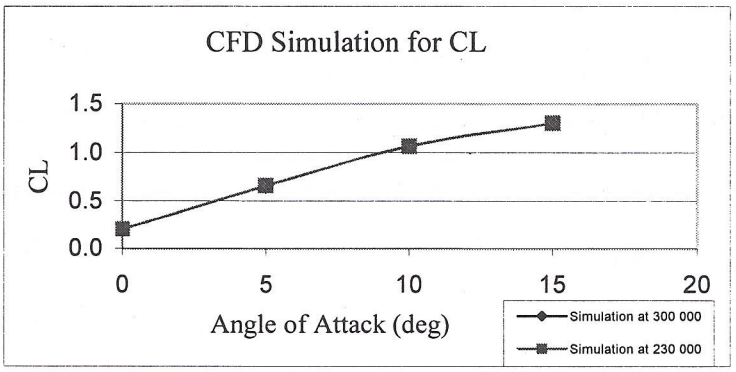

Figure 6: CFD simulation for CL

From figure 6, it can be seen that the deviation between the two is only about 1%, meaning the results are free from the elements factor. Figure 7 shows an example of simulations at 15^0 and 0^0 angles of attack at 230, 000 meshing elements.

Beside the simulation with k-epsilon standard, the simulation was also conducted at k-epsilon RNG. Figure 8 shows a comparison of the lift coefficient for k-epsilon standard and k-epsilon RNG. Simulation 1 and 2 represent the lift coefficient for k-epsilon with 230,000 and 300,000 elements respectively whereas

simulation 3 and 4 are the results for k-epsilon RNG with respect to the same amount of elements. Figure 8 shows that the lift coefficient is slightly bigger in average by using k-epsilon RNG compared to the k-epsilon standard. However, since the difference is small, the results can be accepted.

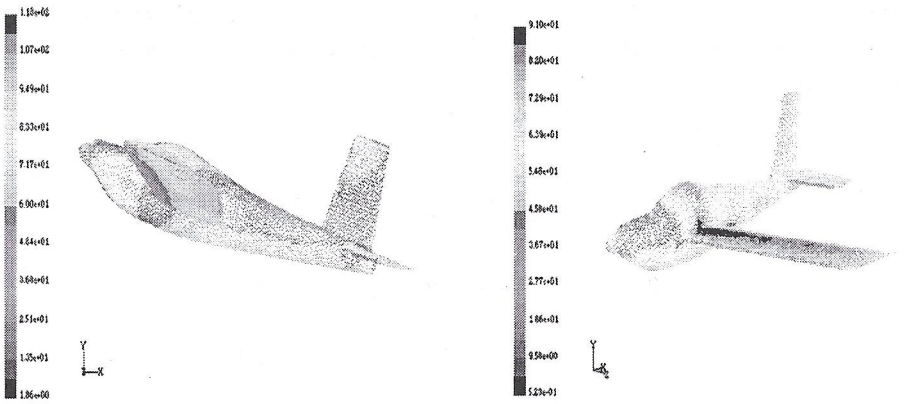

Figure 7: Simulation study at 15^0 and 0^0 angle of attack

Angle of Attack	C_L			
	Simulation1 230k elements k-epsilon	Simulation2 300k elements k-epsilon	Simulation3 230k elements k-epsilon RNG	Simulation4 300k elements k-epsilon RNG
0°	0.1990	0.2016	0.2025	0.2041
5°	0.6588	0.6601	0.6689	0.6695
10°	1.0649	1.0611	1.0805	1.0782
15°	1.2985	1.2983	1.2918	1.2738

Figure 8: Lift coefficients for k-epsilon and k-epsilon RNG

The wing and fuselage velocity profiles were then analysed, with simulation results at the speed of 70 m/s and angle of attack of 5^0 was discussed. Figure 9 shows a velocity profile on the wing. The highest speed achieved on the upper

surface of the wing was 90.97 m/s located about 10% from the leading edge. The speed decreased as it moved from the leading edge to the trailing edge. The lowest speed was recorded at 42.81 m/s about at the trailing edges on the upper surface. Unsteady flow and stall phenomenon might occur surrounding this location. The flow over the lower surface of the wing showed that a velocity profile is increased when it moved from leading edge to trailing edge.

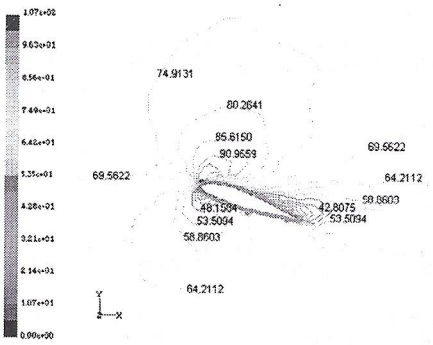

Figure 9: Velocity profile on wing

Figure 10 is the velocity profile on the centre of the fuselage at 70 m/s. From this simulation it was found that the speed at the bottom front of this aircraft was only about 58 m/s. Behind the aircraft, the speed was only around 48.16 m/s, this might be caused by the flow that had been saturated and the generated vortex flow at this particular location.

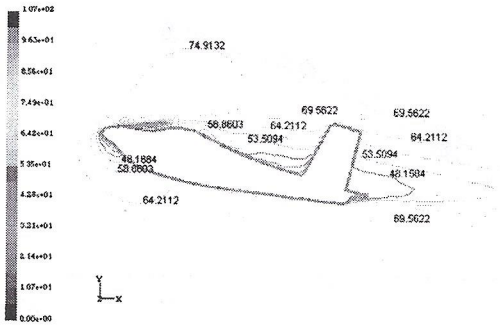

Figure 10: Velocity profile on fuselage

4.0 RESULTS

4.1 Lift Coefficient

Figure 11 shows a comparison results for the lift coefficient obtained from both studies in this project. Experimental study at IAR–NRC showed that this aircraft stalled at 15^0 angle of attack and equivalent to C_{Lmax} of 1.09, whereas C_{Lmax} was

found to be 1.05 measured by UTM-LST at angle of attack of 16^0. The coefficient of lift was found to be slightly higher by CFD study. For example at 15^0, CFD depicts the coefficient of lift was about 1.29° whereas IAR-NRC and UTM–LST showed 1.09° and 1.04° respectively. However, the slopes were in agreement to each other.

Angle of Attack	C_L					
	IAR - NRC	UTM-LST	Simulation 1	Simulation 2	Simulation 3	Simulation 4
0°	0.24	0.17	0.1990	0.2016	0.2025	0.2041
5°	0.64	0.58	0.6588	0.6601	0.6689	0.6695
10°	0.92	0.88	1.0649	1.0611	1.0805	1.0782
15°	1.09	1.04	1.2985	1.2983	1.2918	1.2738

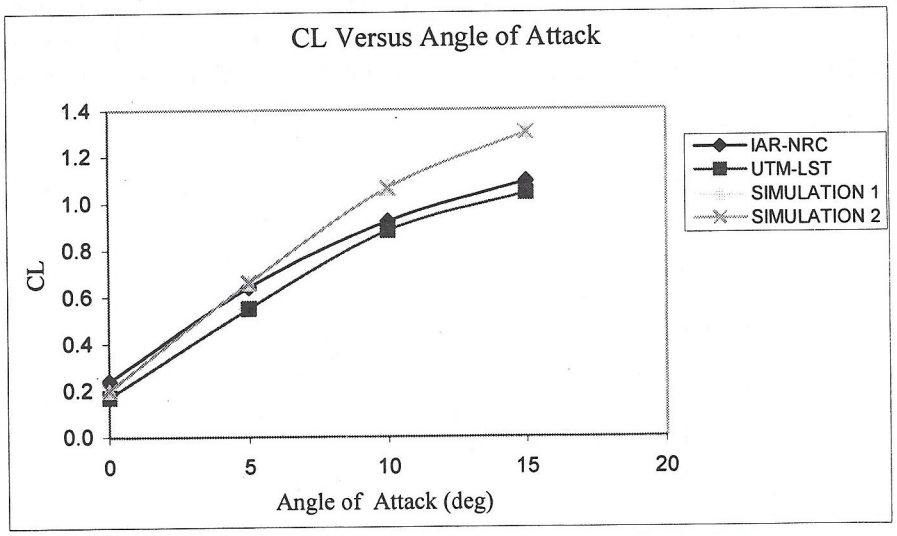

Figure 11: Profile of lift coefficient

4.2 Drag Coefficient

Figure 12 shows the profile of drag coefficient of this aircraft. From the experimental study at IAR/NRC, the drag coefficient was 0.23 compared to 0.2 measured by UTM-LST at 15^0angle of attack. This shows that the drag measured by both tunnels was in agreement to each other at low angle of attack. Figure 12 also depicts that the drag coefficient was slightly higher by CFD study compared to the experimental works. For example, at zero angle of attack, C_D obtained by

CFD was around 0.08 compared to 0.03 from the experiment. This small deviation might be due to the inaccuracy and imperfection of the CFD model.

Alpha	C_D					
	IAR - NRC	UTM-LST	Simulation 1	Simulation 2	Simulation 3	Simulation 4
0°	0.031	0.030	0.0869	0.0866	0.0749	0.0749
5°	0.060	0.050	0.1256	0.1249	0.1101	0.1097
10°	0.121	0.120	0.2149	0.2149	0.1933	0.1930
15°	0.230	0.200	0.3585	0.3473	0.3285	0.3254

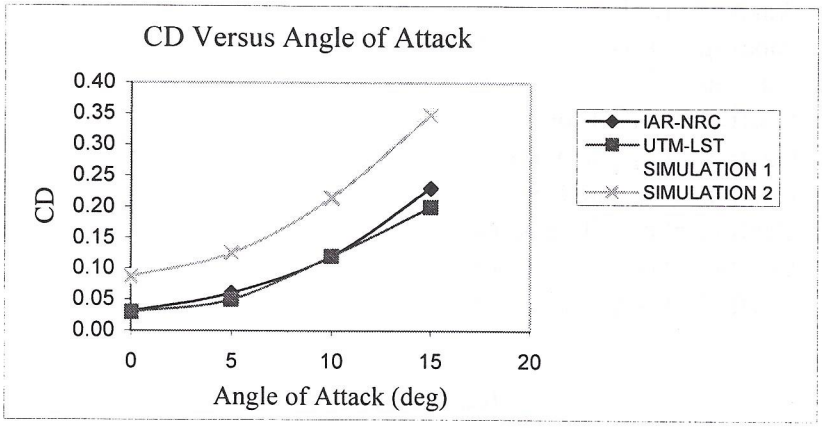

Figure 12: Profile of drag coefficient

5.0 RECOMMENDATION

It can be seen that the results from experimental and simulation were in agreement except at high angle of attack. The difference is believed mainly due to the contribution of the discrepancy of the CFD model. Inaccuracy and imperfection of the 3-dimensional aircraft solid drawing for CFD simulation have influenced the results. In future, capturing and digitising the scan image of aircraft model using a software called Photomodeller Pro 3.0 might be advantageous. By this, it is hoped that a real image of the aircraft model will be obtained.

6.0 CONCLUSION

Throughout this paper, the procedures and result of the experimental and simulation studies have been presented. Results for the lift coefficient showed that both studies were in agreement especially at a low angle of attack. Nevertheless, CFD simulation showed that the drag coefficient was slightly higher than experimental. For the STI corrections, gathering data at high intermediate angles (+ve and –ve) might be advantageous.

ACKNOWLEDGEMENTS

1) Institute Aerodynamic Research, National Research Council, IAR–NRC, Ottawa, Canada.
2) SME Aerospace, Kuala Lumpur, Malaysia.

NOMENCLATURE

α	Angle of attack
ε	Blockage correction
ρ	Air density
C_L	Coefficient of lift force
C_D	Coefficient of drag force
C_Y	Coefficient of side force
C_l	Coefficient of rolling moment
C_m	Coefficient of pitching moment
C_n	Coefficient of yawing moment

REFERENCES

1. Barlow, J.B., et al, 1999, *Low Speed Wind Tunnel Testing,* 3rd edition, New York: A Wiley–Interscience Publication.
2. Pope, A., M.S., 1954, *Wind Tunnel Testing,* 2nd Edition, New Jersey–PrenticeHall.
3. Katz, J. and Plotkin, A., 1991, *Low Speed Aerodynamic from wing Theory To Panel Methods* , New York:McGraw Hill Inc.
4. John, A.D., 1995, *Computational Fluid Dynamics–The Basics with Applications*, New York:McGraw Hill Inc.
5. Singhal, A.K., 1998, *Key Elements of Verification and Validation of CFD Software,* Hustville, AL , CFD Research Corporation.
6. Zan, S.J., 2002, *Overview of Data Reduction Procedures for 3-D Aircraft Model Testing in the Universiti Teknologi Malaysian Wind Tunnel.*